Passive Target Motion Analysis by Fusion of Linear Arrays and Sonobuoys in a Cluttered Environment

Jérémy Payan, Antoine Lebon, Annie-Claude Perez, Dann Laneuville, Claude Jauffret

Passive Target Motion Analysis by Fusion of Linear Arrays and Sonobuoys in a Cluttered Environment

Jérémy Payan*†, Antoine Lebon*†, Annie-Claude Pérez*, Claude Jauffret*, Dann Laneuville†

***Abstract*—This paper is devoted to the analysis of the motion of a target using information from two kinds of cooperative maritime sensors: A wireless network of sonobuoys detecting a signal emitted by a source in motion with constant velocity; Vertical antennas measuring the cosine of the elevation angles of the received signal. We prove that the trajectory of the source is observable, under non-restrictive assumptions concerning the scenario. After thresholding, the data are surrounded by false alarms; therefore, a probabilistic data association model is employed. The joint exploitation of the measurements of the time differences of arrival together with the measurements of the cosines of the elevation angles allow estimating the trajectory of the source. The empirical performance of the maximum likelihood estimator (MLE), evaluated by extensive simulations, reaches the asymptotic performance given by the Cramér–Rao lower bound. Finally, we extend our study to the case where the energy of the data is available, after thresholding. Again, the MLE is efficient and its performance is significantly improved.**

***Index Terms*—Fisher information matrix, multipath, observability, probabilistic data association with maximum likelihood estimation (ML-PDA), sonobuoy, target motion analysis, time difference of arrival (TDOA), vertical array.**

I. Introduction

In this paper, we are concerned with passive three-dimensional submarine target tracking. Passive target tracking consists of estimating the parameters that define the trajectory of the target, from sensors which do not emit any signal. Each sensor receives the signal emitted by the moving target. Passive target tracking is of significant importance in coastal waters or submarine surveillance systems [1].

Passive target tracking may be performed by using one sensor, for example in [2], but a network of sensors may also be used. Generally, the sensors are spatially separated from each other. Then, different kinds of sensors may be used in the network. We will focus specifically on two of them: vertical linear arrays and sonobuoys [3]. Sonobuoys measure the time difference of arrival (TDOA) between the signal originated by the target and that originated by a reference sonobuoy [4]. The measurements acquired by a vertical linear array are the cosines of the elevation angles of the target originated wave.

Each of these two kinds of sensors has its own advantages and disadvantages regarding the asymptotic performance of the estimation. The asymptotic performance is given by the Cramér–Rao lower bound (CRLB) [5]. Due to their rather similar depths, the sonobuoys are very unlikely to estimate the depth of the target with relatively low variance [6], unless there is a large number of sonobuoys. But vertical linear arrays can estimate the target depth with low variance. In view of these considerations, it would be interesting to combine the measurements coming from both kinds of sensors, to obtain 'the best of both worlds', especially for the estimation of the three-dimensional position vector. By merging these different kinds of sensors, we obtain what we call a 'mixed sensor network'.

In a realistic situation, a detection step is applied to the raw data. One then has to deal with a cluttered environment due to background noise during the tracking. The tracking may then be carried out using the probabilistic data association (PDA) algorithm [2], [7], [8], which takes into account the presence of false alarms (which compose the clutter), as well as a non-unity detection probability. It is then possible to estimate the parameters of interest when true detections are drowned in false alarms and do not surely appear at each sampling time. In our study, we will use the PDA with maximum likelihood estimation (ML-PDA) [2], [9], [10]. ML-PDA is a batch technique using all available measurements at once. It has been shown that this technique allows the construction of statistically efficient estimators [2], [9]. Later, an extension to the ML-PDA technique using the amplitude information (AI) of each detection was created [11], [12]. It allows tracking in situations with very low signal-to-noise ratio (SNR).

With all these considerations, the computation of a maximum likelihood estimator to achieve the target tracking in a passive sensor network will be discussed. We place ourselves in a realistic context due to the statistical assumptions of the ML-PDA. We use both the PDA techniques mentioned above: ML-PDA and ML-PDA with AI. Our paper has 6 main sections. Section II formulates the problem as well as the notation to be used. In Section III, the observability is detailed. Section IV outlines the interest of the sensor fusion by determining the relevant asymptotic performances. Section V presents briefly the ML-PDA technique. Section VI presents some numerical results. Then follow the Conclusion, appendices, and reference list.

II. Problem Formulation and Notations

The mixed sensor network is composed of N_S sonobuoys located on the surface of the sea and N_A vertical linear arrays. At each sampling time $k = 1 : K$, each sonobuoy gets the TDOA of the target signal with respect to a chosen reference sonobuoy. This may be expressed as a range difference, by

*Université de Toulon, Aix Marseille Univ, CNRS, IM2NP, Toulon, France, CS 60584, 83041 TOULON Cedex 9, France
(Email: jeremy-payan, antoine-lebon@etud.univ-tln.fr, annie-claude.perez, jauffret@univ-tln.fr)
†dann.laneuville@naval-group.com

assuming a constant speed in the sea. Each linear array measures the cosine of the elevation angle: the angle between the direct path and the reflected path. We assume that the waves propagate in straight lines and are only reflected once [13], [14]. The reflected path corresponds to the reflection from the seabed. The positions of the sensors in the network are uniformly distributed over a square. However, each position is exactly known and the sensors are motionless during the whole acquisition time.

The target is supposed to travel at a constant velocity (CV) and at a constant depth. Consequently, the state vector defining the target trajectory is given by

$$X^T = (x; y; z; \dot{x}; \dot{y}) \tag{1}$$

where $(x; y; z)$ is the initial position (given in meters) in a 3-dimensional Cartesian space and $(\dot{x}; \dot{y})$ is the velocity of the target (given in meters per second) in the horizontal plane. So, we may define the target position at each sampling time $k = 1 : K$ with respect to X:

$$\begin{bmatrix} x_k \\ y_k \\ z_k \end{bmatrix} = \begin{bmatrix} 1 & 0 & 0 & k\Delta t & 0 \\ 0 & 1 & 0 & 0 & k\Delta t \\ 0 & 0 & 1 & 0 & 0 \end{bmatrix} X \tag{2}$$

with Δt being the sampling period. Note that $z_k = z$.

Now we can specify the measurements acquired by each sensor. Each sonobuoy is located at the coordinates $(x_i^S; y_i^S; z_i^S)$, where $z_i^S = 0$. $r_{i,k}$ is the range between the target and the sonobuoy i at sampling time k:

$$r_{i,k} = \sqrt{\left(x_k - x_i^S\right)^2 + \left(y_k - y_i^S\right)^2 + z^2} \tag{3}$$

Then we get

$$\Delta r_{i,k} = r_{i,k} - r_{i_0,k} + \varepsilon_{i,k} \tag{4}$$

$\Delta r_{i,k}$ is the measurement coming from the sonobuoy i at sampling time k. i_0 denotes the reference sonobuoy[1], and $\varepsilon_{i,k}^S$ is a zero-mean additive white Gaussian noise of standard deviation σ_Δ. The measurements collected by the vertical arrays are the following:

$$\begin{aligned} c_{n,k}^D &= \cos\left(\phi_{n,k}^D\right) + \varepsilon_{n,k}^D \\ &= \frac{z - z_n^A}{\sqrt{(x_k - x_n^A)^2 + (y_k - y_n^A)^2 + (z - z_n^A)^2}} + \varepsilon_{n,k}^D \end{aligned} \tag{5}$$

$$\begin{aligned} c_{n,k}^B &= \cos\left(\phi_{n,k}^B\right) + \varepsilon_{n,k}^B \\ &= \frac{2z_B - (z_n^A + z)}{\sqrt{(x_k - x_n^A)^2 + (y_k - y_n^A)^2 + (z + z_n^A - 2z_B)^2}} + \varepsilon_{n,k}^B \end{aligned} \tag{6}$$

Equation (5) defines the measurement coming from the direct path, whereas (6) refers to the reflected one. Both are relative to antenna n at sampling time k. Each antenna is located at the coordinates $(x_n^A; y_n^A; z_n^A)$, z_n^A being the acoustic center and z_B being the depth of the seabed. $\varepsilon_{n,k}^D$ and $\varepsilon_{n,k}^B$ are zero-mean additive white Gaussian noises of standard deviation σ_A. Figure 1 illustrates the elevation angles of the target.

[1]We arbitrarily choose the nearest sonobuoy from the center of the network as the reference.

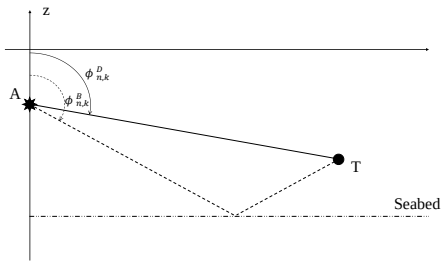

Fig. 1. Elevations of the direct path and of the reflected path.

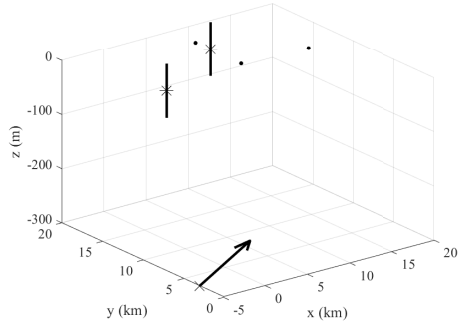

Fig. 2. Example of a mixed-sensor network. Dots: sonobuoys. Vertical lines: linear arrays. Stars: Acoustic center of linear array. Arrow: Target.

Note that the propagation delay is neglected in this study (this assumption was made in [4], [6]).

In the rest of the paper, we will consider a network composed of $N_S = 3$ sonobuoys and $N_A = 2$ vertical linear arrays. The locations of the sensors are uniformly distributed in a square with sides of length 20 km. The number of sampling times is $K = 100$ and the sampling period is $\Delta t = 4$ s. We will consider two cases of the target velocity: a slow target linked to the true state X_L and a fast target linked to X_H. The true states are the following:

$$X_L^T = (-5000; 3000; -300; 4; 3) \tag{7}$$

$$X_H^T = (-5000; 3000; -300; 25; 12) \tag{8}$$

The standard deviation of the measurements coming from the sonobuoys is $\sigma_\Delta = 30$ meters, corresponding to a trade-off between pessimistic [4] and optimistic [15] cases. The standard deviation of the measurements collected by the antennas is $\sigma_A = 0.017$ (implying a standard deviation of the angle greater than 1 degree[2]) The acoustic center of the linear arrays z_n^A is supposed to be 50 m deep. The depth of the seabed z_B is assumed to be -2000 m.

Fig. 2 depicts an example of the sensor network as well as the target track, for the fast target defined above.

[2]For a measurement $m = \cos(\alpha) + \varepsilon_m$, the corresponding standard deviation of α is approximatively $\sigma(\alpha) = \frac{\sigma(m)}{|\sin(\alpha)|}$.

III. Analysis of Observability

The following analysis will be conducted step-by-step.

First, we suppose there are only two vertical antennas. For the sake of simplicity, the two antennas are located at $\left(0; y^A; z^A\right)^T$ and $\left(0; -y^A; z^A\right)^T$. For convenience, we define $A_1 = (0; y_A)$ and $A_2 = (0; -y_A)$. The noise-free measurements collected by them, i.e. $\left(\cos\left(\Phi^D_{1,k}\right), \cos\left(\Phi^D_{2,k}\right)\right)$ and $\left(\cos\left(\Phi^B_{1,k}\right), \cos\left(\Phi^B_{2,k}\right)\right)$, correspond to the state vector $X^T = (x, y, z, \dot{x}, \dot{y})$, and the one defining the trajectory of a ghost target, say $X^T_G = (-x, y, z, -\dot{x}, \dot{y})$. The trajectory is then observable up to the axial symmetry around the axis $(0; y)$.

Now, we add two sonobuoys allowing us to measure the time differences of arrival (TDOA). We define $S_1 = (x^S_1; y^S_1)$ and $S_2 = (x^S_2; y^S_2)$. The question is: do these new measurements eliminate the ghost? To answer this question, we adopt the approach proposed in [16], i.e. the measurements are taken in continuous time:

$$r_1(t) = \sqrt{\left(x(t) - x^S_1\right)^2 + \left(y(t) - y^S_1\right)^2 + z^2} \tag{9}$$

$$r_2(t) = \sqrt{\left(x(t) - x^S_2\right)^2 + \left(y(t) - y^S_2\right)^2 + z^2} \tag{10}$$

$$r_{G,1}(t) = \sqrt{\left(x(t) + x^S_1\right)^2 + \left(y(t) - y^S_1\right)^2 + z^2} \tag{11}$$

$$r_{G,2}(t) = \sqrt{\left(x(t) + x^S_2\right)^2 + \left(y(t) - y^S_2\right)^2 + z^2} \tag{12}$$

Suppose that $r_1(t) - r_2(t) = r_{G,1}(t) - r_{G,2}(t)$. Then

$$\begin{aligned} &[r_1(t) - r_2(t)]^2 = [r_{G,1}(t) - r_{G,2}(t)]^2 \\ &\Leftrightarrow r_1^2(t) + r_2^2(t) - 2r_1(t)r_2(t) \\ &= r_{G,1}^2(t) + r_{G,2}^2(t) - 2r_{G,1}(t)r_{G,2}(t) \end{aligned} \tag{13}$$

$$\Leftrightarrow 2\left(x^S_1 + x^S_2\right)x(t) = r_{G,1}(t)r_{G,2}(t) - r_1(t)r_2(t) \tag{14}$$

We deduce from (14) two remarks:

- The difference $r_{G,1}(t)r_{G,2}(t) - r_1(t)r_2(t)$ is a polynomial function.
- Clearly, $r_1(t)r_2(t)$ is a polynomial function iff $r_{G,1}(t)r_{G,2}(t)$ is a polynomial function.

Our analysis is based on this remark. We examine if the existence of a ghost target is compatible with the different assumptions discussed in the following.

Discussion:

A. $x^S_1 + x^S_2 \neq 0$

Multiplying the terms of (14) by $r_{G,1}(t)r_{G,2}(t) + r_1(t)r_2(t)$ we get

$$\begin{aligned} &\left[r_{G,1}(t)r_{G,2}(t) + r_1(t)r_2(t)\right]x(t) \\ &= \frac{\left[r_{G,1}(t)r_{G,2}(t)\right]^2 - \left[r_1(t)r_2(t)\right]^2}{2\left(x^S_1 + x^S_2\right)} \end{aligned} \tag{15}$$

Hence, $\left[r_{G,1}(t)r_{G,2}(t) + r_1(t)r_2(t)\right]x(t)$ is a polynomial.

1) $\dot{x} = 0, x \neq 0$, i.e. $x(t) = x \neq 0$: From (14), we have that $r_{G,1}(t)r_{G,2}(t) - r_1(t)r_2(t)$ is a polynomial, and $r_{G,1}(t)r_{G,2}(t) + r_1(t)r_2(t)$ as well by (15). This implies that $r_1(t)r_2(t)$ and $r_{G,1}(t)r_{G,2}(t)$ are two polynomials of degree 2. We define now three other polynomials (of degree 2):

$$\begin{aligned} P(t) &\triangleq r_1^2(t) \\ Q(t) &\triangleq r_2^2(t) \\ R(t) &\triangleq r_1(t)r_2(t) \end{aligned} \tag{16}$$

We have $R^2 = PQ$, which is equivalent to $\frac{R^2}{PQ} = 1$. Hence P and Q divide R. Since the degree of these three polynomials is equal to 2, there is a non-zero number, say α, such that $P = \alpha R$ and $Q = \frac{1}{\alpha}R$. We deduce that $P = \alpha^2 Q$. The coefficient of t^2 is equal to $\dot{y}^2$ in P and in Q. Hence $\alpha^2 = 1$. Consequently, $P = Q$. Now the equality $P - Q = 0$ is equivalent to

$$\begin{aligned} &\left(2y - y^S_1 - y^S_2 + 2t\dot{y}\right)\left(y^S_1 - y^S_2\right) \\ &+ \left(2x - x^S_1 - x^S_2 + 2t\dot{x}\right)\left(x^S_1 - x^S_2\right) = 0 \\ &\Leftrightarrow \begin{cases} y^S_1 = y^S_2 \\ \text{and} \\ x^S_1 = x^S_2 \text{ or } x = \frac{x^S_1 + x^S_2}{2} \end{cases} \end{aligned} \tag{17}$$

The case where $x^S_1 = x^S_2$ and $y^S_1 = y^S_2$ must be discarded since the sonobuoys are not in the same place. Hence, we retain $y^S_1 = y^S_2$ and

$$x = \frac{x^S_1 + x^S_2}{2} \tag{18}$$

Now, if we define three new polynomials

$$\begin{aligned} P_G(t) &\triangleq r_{G,1}^2(t) \\ Q_G(t) &\triangleq r_{G,2}^2(t) \\ R_G(t) &\triangleq r_{G,1}(t)r_{G,2}(t) \end{aligned} \tag{19}$$

and if we carry out similar computations, we obtain

$$x = -\frac{x^S_1 + x^S_2}{2} \tag{20}$$

Equalities (18) and (20) are incompatible. We conclude that when $x^S_1 + x^S_2 \neq 0$, the trajectory of the source is observable.

2) $\dot{x} \neq 0$, i.e. $x(t) = x + t\dot{x}$: First, from (14), we deduce that $r_{G,1}(t)r_{G,2}(t) - r_1(t)r_2(t)$ is a polynomial. Let us rewrite $x(t)$ as $x(t) = (t - t^*)\dot{x}$, with $t^* = -\frac{x}{\dot{x}}$

$$\begin{aligned} (15) \Leftrightarrow &2(t - t^*)\left(x^S_1 + x^S_2\right)\left[r_{G,1}(t)r_{G,2}(t) + r_1(t)r_2(t)\right]\dot{x} \\ &= \left[r_{G,1}(t)r_{G,2}(t)\right]^2 - \left[r_1(t)r_2(t)\right]^2 \end{aligned} \tag{21}$$

The time t^* is hence a zero of the polynomial $\left[r_{G,1}(t)r_{G,2}(t)\right]^2 - \left[r_1(t)r_2(t)\right]^2$. It can be written as $\left[r_{G,1}(t)r_{G,2}(t)\right]^2 - \left[r_1(t)r_2(t)\right]^2 = (t - t^*)S(t)$, where $S(t)$ is a polynomial. Equality (21) gives us

$$r_{G,1}(t)r_{G,2}(t) + r_1(t)r_2(t) = \frac{1}{2\dot{x}\left(x^S_1 + x^S_2\right)}S(t) \tag{22}$$

We deduce from (22) that $r_{G,1}(t)r_{G,2}(t)+r_1(t)r_2(t)$ is again a polynomial. Hence $r_{G,1}(t)r_{G,2}(t)$ and $r_1(t)r_2(t)$ are both polynomials.

The same reasoning as in 1) yields again the equalities $P = Q$, which is equivalent to

$$\begin{cases}(x-x_1^S)^2+(y-y_1^S)^2+z^2 = (x-x_2^S)^2+(y-y_2^S)^2+z^2\\ 2(x-x_1^S)\dot{x}+2(y-y_1^S)\dot{y} = 2(x-x_2^S)\dot{x}+2(y-y_2^S)\dot{y}\end{cases}$$
$$\Leftrightarrow \begin{cases}(2x-x_1^S-x_2^S)(x_1^S-x_2^S)+(2y-y_1^S-y_2^S)(y_1^S-y_2^S)=0\\ (x_1^S-x_2^S)\dot{x}+(y_1^S-y_2^S)\dot{y}=0\end{cases} \tag{23}$$

We also get $P_G = Q_G$, which is equivalent to

$$\begin{cases}(-2x-x_1^S-x_2^S)(x_1^S-x_2^S)+(2y-y_1^S-y_2^S)(y_1^S-y_2^S)=0\\ -(x_1^S-x_2^S)\dot{x}+(y_1^S-y_2^S)\dot{y}=0\end{cases} \tag{24}$$

Equations (23) and (24) can be rewritten as the following system

$$\begin{bmatrix}2(x_1^S-x_2^S) & 2(y_1^S-y_2^S) & 0 & 0\\ -2(x_1^S-x_2^S) & 2(y_1^S-y_2^S) & 0 & 0\\ 0 & 0 & (x_1^S-x_2^S) & (y_1^S-y_2^S)\\ 0 & 0 & -(x_1^S-x_2^S) & (y_1^S-y_2^S)\end{bmatrix}\begin{bmatrix}x\\y\\\dot{x}\\\dot{y}\end{bmatrix}$$
$$= \begin{bmatrix}(x_1^S)^2-(x_2^S)^2+(y_1^S)^2-(y_2^S)^2\\ (x_1^S)^2-(x_2^S)^2+(y_1^S)^2-(y_2^S)^2\\ 0\\ 0\end{bmatrix} \tag{25}$$

Because the target is moving (since $\dot{x} \neq 0$), the determinant of the above matrix, which is $16\left[(x_1^S-x_2^S)(y_1^S-y_2^S)\right]^2$, must be zero (otherwise $\dot{x} = \dot{y} = 0$).

We have hence to consider two possibilities: either $x_1^S = x_2^S$ or $y_1^S = y_2^S$ (we cannot have simultaneously the two equalities, since the sonobuoys are not collocated). If $x_1^S = x_2^S$, then $y = \frac{y_1^S+y_2^S}{2}$ and $\dot{y} = 0$. In this case, the trajectory of the target is not observable since the two vectors $X^T = \left(x, \frac{y_1^S+y_2^S}{2}, z, \dot{x}, 0\right)$ and $X_G^T = \left(-x, \frac{y_1^S+y_2^S}{2}, z, -\dot{x}, 0\right)$ give the same measurements.

If $y_1^S = y_2^S$, then $x = \frac{x_1^S+x_S^2}{2}$ and $\dot{x} = 0$. This must be discarded.

B. $x_1^S + x_2^S = 0$

1) $x_1^S = x_2^S = 0$: The measurements are

$$r_1(t) = \sqrt{x^2(t)+\left(y(t)-y_1^S\right)^2+z^2} = r_{G,1}(t) \tag{26}$$

$$r_2(t) = \sqrt{x^2(t)+\left(y(t)-y_2^S\right)^2+z^2} = r_{G,2}(t) \tag{27}$$

The two state vectors X and X_G give the same measurements. The trajectory of the target is unobservable.

2) $x_1^S = -x_2^S \neq 0$: The measurements are

$$r_1(t) = \sqrt{\left(x(t)-x_1^S\right)^2+\left(y(t)-y_1^S\right)^2+z^2} \tag{28}$$

$$r_2(t) = \sqrt{\left(x(t)+x_1^S\right)^2+\left(y(t)-y_2^S\right)^2+z^2} \tag{29}$$

$$r_{G,1}(t) = \sqrt{\left(x(t)+x_1^S\right)^2+\left(y(t)-y_1^S\right)^2+z^2} \tag{30}$$

$$r_{G,2}(t) = \sqrt{\left(x(t)-x_1^S\right)^2+\left(y(t)-y_2^S\right)^2+z^2} \tag{31}$$

And, from (14), we have $r_{G,1}(t)r_{G,2}(t) - r_1(t)r_2(t) = 0$, i.e. $\frac{r_1(t)r_2(t)}{r_{G,1}(t)} = r_{G,2}(t)$, which implies that $\left(\frac{r_1(t)r_2(t)}{r_{G,1}(t)}\right)^2 = r_{G,2}^2(t)$, i.e. $\frac{PQ}{P_G} = Q_G$ (with the definitions (16) and (19)).

Note that the two polynomials $P(t) = \left(x(t)-x_1^S\right)^2 + \left(y(t)-y_1^S\right)^2+z^2$ and $P_G(t) = \left(x(t)+x_1^S\right)^2+\left(y(t)-y_1^S\right)^2+z^2$ are coprime. Hence, thanks to the Gauss Lemma, P_G divides Q. Because they have the same degree, there is a real non-zero number, say β, such that $P_G = \beta Q$. Consequently, $P = \beta Q_G$. The coefficients of t^2 in P_G and βQ being equal, we deduce that $\beta = 1$. Consequently, $r_1(t) = r_{G,2}(t)$ and $r_2(t) = r_{G,1}(t)$, which implies that $r_1(t) - r_2(t) = -\left[r_{G,1}(t) - r_{G,2}(t)\right]$. Hence, the two state vectors X and X_G do not give the same measurements. The trajectory of the target is observable.

Now, we can summarize this discussion by the following theorem

Theorem 1:

- If the line (S_1, S_2) is not in the vertical plane containing A_1 and A_2, then the trajectory of any target travelling in this axis is observable. Otherwise, the trajectory of any target travelling out of this axis is observable up to the axial symmetry around this line.
- If the lines (A_1, A_2) and (S_1, S_2) are parallel, but not contained in the same vertical plane, then the trajectory of any target travelling in the perpendicular bisector of $[S_1, S_2]$ is observable up to the axial symmetry around the line (A_1, A_2).
- In any other cases, the trajectory of the target is observable.

Consequence: If we have three sonobuoys forming a triangle, the trajectory of any target is observable.

IV. Asymptotic Performance

In this section, we present the main concern about the fusion of the sensors in the sense of the asymptotic performance. The asymptotic performances are known from the Cramér–Rao Lower Bound (CRLB), or, similarly, from the Fisher Information Matrix (FIM). We recall the link between the CRLB for unbiased estimators and the FIM:

$$B = F^{-1} \tag{32}$$

where F is the FIM and B is the CRLB for unbiased estimators.

First, we show the expressions for the FIM in a clean environment for each kind of sensor:

TABLE I
EMPIRICAL MEAN VALUES OF THE DIAGONAL ELEMENTS OF THE FISHER INFORMATION MATRICES

Component	Unit	Sonobuoys	Antennas	Mixed network
x	m^{-2}	0.0111	2.88×10^{-4}	0.0114
y	m^{-2}	0.0457	7.92×10^{-5}	0.0457
z	m^{-2}	3.78×10^{-5}	6.8×10^{-3}	6.9×10^{-3}
$\dot{x}$	$\mathrm{m}^{-2}.\mathrm{s}^2$	614.48	17.16	631.63
$\dot{y}$	$\mathrm{m}^{-2}.\mathrm{s}^2$	2583.5	4.97	2588.4

$$F_\Delta = \sum_{\substack{i=1\\ i\neq i_0}}^{N_S}\sum_{k=1}^{K}\frac{1}{\sigma_\Delta^2}\left[\nabla_X r_{i,k}-\nabla_X r_{i_0,k}\right]\left[\nabla_X r_{i,k}-\nabla_X r_{i_0,k}\right]^T \tag{33}$$

$$\begin{aligned}F_A = \sum_{j=1}^{N_A}\sum_{k=1}^{K}\frac{1}{\sigma_A^2}\Big[&\nabla_X\cos\left(\phi_{j,k}^D\right)\nabla_X^T\cos\left(\phi_{j,k}^D\right)\\ &+\nabla_X\cos\left(\phi_{j,k}^B\right)\nabla_X^T\cos\left(\phi_{j,k}^B\right)\Big]\end{aligned} \tag{34}$$

F_Δ and F_A are then the FIMs for the sonobuoys and linear arrays, respectively. The FIM F after the fusion of the sensors is then

$$F = F_\Delta + F_A \tag{35}$$

To illustrate the benefit of fusing the sensors, the following procedure is applied. For the slow target and the numerical values defined in Section II, 5000 random mixed sensors networks are created. Indeed, we recall that the positions of the sensors are uniformly distributed in a square with sides of length 20 km. For each network, F_Δ, F_A and F are computed. Then, the empirical mean value of the diagonal elements of each FIM is extracted to allow the comparison. The result is shown in Table I.

It is noticeable that the amount of information coming from the sonobuoys on the depth of the target is very poor. But the other components would be estimated accurately. On the other hand, the linear arrays do not bring much information about the position in the plane nor on the velocity of the target, compared to the sonobuoys. But, the amount of information on the depth is rather important. Then, the mixed sensor network benefits from the best of both kinds of sensors, and thus allows an accurate estimation of the whole state vector.

Let us note that in some cases where the linear arrays are too distant, the gain of information on the depth of the target may be negligible.

V. THE PROBABILISTIC DATA ASSOCIATION MODEL

A. Statistical Assumptions of the Probabilistic Data Association Model

1) General Case: The consideration of a cluttered environment is justified by the technological roughness of the sonobuoys. These sensors cannot embed a sophisticated and complex signal processing chain. Thus, these sensors alone cannot extract the target-originated measurements.

The classic scenario is the following: a sensor gets at time k a collection $s_k = (s_{1,k}, \cdots s_{m_k,k})^T$ of measurements. Some statistical assumptions are necessary to formulate an ML-PDA model. Following [2], [8], these are:

- The vectors s_k are independent conditionally on X for $k = 1 : K$.
- The detections due to the target are corrupted by a zero-mean additive white Gaussian noise. The power of the noise is σ^2 (a subscript, A or Δ, will be added when applied to the mixed sensor network). These detections are called 'true detections'.
- The clutter is composed of the false alarms and is distributed according to an uniform law over a scan space u.
- The number of false alarms at a specific sample k follows a Poisson law μ_{fa} of parameter λu (the expected number of false alarms).
- True detections appear at most once at each sampling time, with a detection probability P_d.

It is then possible to express the likelihood of X given s_k, due to the total probability theorem:

$$\begin{aligned}L(X|s) = \prod_{k=1}^{K}\Bigg\{&\frac{1-P_d}{u^{m_k}}\mu_{fa}(m_k) + \frac{P_d}{u^{m_k-1}}\frac{\mu_{fa}(m_k-1)}{m_k}\\ &\times\sum_{i=1}^{m_k}\frac{1}{\sqrt{2\pi}\sigma}\exp\left[-\frac{1}{2}\left(\frac{s_{i,k}-h_k(X)}{\sigma}\right)^2\right]\Bigg\}\end{aligned} \tag{36}$$

with h_k the state model at time k.

2) Extension to the Use of Amplitude Information: The ML-PDA model using AI was introduced in [11], [12]. All the previously stated assumptions still hold. The amplitude associated with each detection is then considered. In a similar manner to the previous part and with the same notation, we may express the likelihood of X given s_k:

$$\begin{aligned}L(X|s,R) = \prod_{k=1}^{K}\Bigg\{&\frac{1-P_d}{u^{m_k}}\mu_{fa}(m_k)\prod_{i=1}^{m_k}p_0^\tau(R_{i,k})\\ &+\frac{P_d}{u^{m_k-1}}\frac{\mu_{fa}(m_k-1)}{m_k}\prod_{i=1}^{m_k}p_0^\tau(R_{i,k})\\ &\times\sum_{i=1}^{m_k}\frac{1}{\sqrt{2\pi}\sigma}\rho_{i,k}\exp\left[-\frac{1}{2}\left(\frac{s_{i,k}-h_k(X)}{\sigma}\right)^2\right]\Bigg\}\end{aligned} \tag{37}$$

with $R_{i,k}$ the amplitude associated with the detection, τ the detection threshold, and

$$p_0^\tau(R_{i,k}) = \frac{1}{P_{fa}}p_0(R_{i,k}) \tag{38}$$

$$p_1^\tau(R_{i,k}) = \frac{1}{P_d}p_1(R_{i,k}) \tag{39}$$

$$\rho_{i,k} = \frac{p_1^\tau(R_{i,k})}{p_0^\tau(R_{i,k})} \tag{40}$$

where p_0 and p_1 are the probability density functions (pdf) associated to the amplitudes under both hypotheses (there is only noise or there is signal and noise, respectively) and P_{fa} is the probability of a false alarm.

B. Application to the Mixed Sensor Network

The general likelihoods under both architectures have been presented. According to the literature [2], [8], [11], [12], the log-likelihood function is chosen as the criterion to be maximized (up to a constant term). The noise is supposed to be independent through the samples and between sensors. The criteria will now be presented by applying the ML-PDA model to our study with the notation described in Section II:

- When the amplitude information is not available, we define the quantities

$$C_1(X|\Delta r_{i,k}) = \log\left\{1 - P_{d\Delta} + \frac{P_{d\Delta}}{\lambda_\Delta} \times \sum_{j=1}^{m_{i,k}} \frac{1}{\sqrt{2\pi}\sigma_\Delta} \exp\left[-\frac{1}{2}\left(\frac{\Delta r_{i,j,k} - r_{i,k} + r_{i_0,k}}{\sigma_\Delta}\right)^2\right]\right\} \tag{41}$$

$$C_2(X|c^D_{l,k}) = \log\left\{1 - P_{dA} + \frac{P_{dA}}{\lambda_A} \times \sum_{j=1}^{m_{l,k}} \frac{1}{\sqrt{2\pi}\sigma_A} \exp\left[-\frac{1}{2}\left(\frac{c^D_{l,j,k} - \cos\left(\phi^D_{l,k}\right)}{\sigma_A}\right)^2\right]\right\} \tag{42}$$

$$C_3(X|c^B_{n,k}) = \log\left\{1 - P_{dA} + \frac{P_{dA}}{\lambda_A} \times \sum_{j=1}^{m_{n,k}} \frac{1}{\sqrt{2\pi}\sigma_A} \exp\left[-\frac{1}{2}\left(\frac{c^B_{n,j,k} - \cos\left(\phi^B_{n,k}\right)}{\sigma_A}\right)^2\right]\right\} \tag{43}$$

where σ^2 is the power of the noise, λ is the expected number of false alarms per unit area, and P_d is the detection probability. The subscript Δ indicates the sonobuoys, and the subscript A indicates the linear arrays.
The criterion to optimize is then

$$C(X) = \sum_{\substack{i=1 \\ i\neq i_0}}^{N_S}\sum_{k=1}^{K} C_1(X|\Delta r_{i,k}) + \sum_{l=1}^{N_A}\sum_{k=1}^{K} C_2(X|c^D_{l,k}) + \sum_{n=1}^{N_A}\sum_{k=1}^{K} C_3(X|c^B_{n,k}) \tag{44}$$

- Similarily, when the amplitude information is available, we define

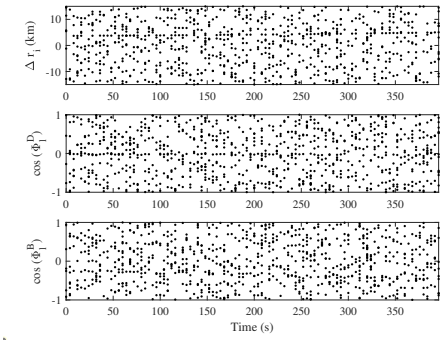

Fig. 3. Measurements obtained for each sensor in one run. $P_d = 0.6$, $\lambda u = 8$.

$$C_1(X|\Delta r_{i,k}, R_{i,k}) = \log\left\{1 - P_{d\Delta} + \frac{P_{d\Delta}}{\lambda_\Delta} \times \sum_{j=1}^{m_{i,k}} \frac{\rho_{i,j,k}}{\sqrt{2\pi}\sigma_\Delta} \exp\left[-\frac{1}{2}\left(\frac{\Delta r_{i,j,k} - r_{i,k} + r_{i_0,k}}{\sigma_\Delta}\right)^2\right]\right\} \tag{45}$$

$$C_2(X|c^D_{l,k}, R^D_{l,k}) = \log\left\{1 - P_{dA} + \frac{P_{dA}}{\lambda_A} \times \sum_{j=1}^{m_{l,k}} \frac{\rho_{l,j,k}}{\sqrt{2\pi}\sigma_A} \exp\left[-\frac{1}{2}\left(\frac{c^D_{l,j,k} - \cos\left(\phi^D_{l,k}\right)}{\sigma_A}\right)^2\right]\right\} \tag{46}$$

$$C_3(X|c^B_{n,k}, R^B_{n,k}) = \log\left\{1 - P_{dA} + \frac{P_{dA}}{\lambda_A} \times \sum_{j=1}^{m_{n,k}} \frac{\rho_{n,j,k}}{\sqrt{2\pi}\sigma_A} \exp\left[-\frac{1}{2}\left(\frac{c^B_{n,j,k} - \cos\left(\phi^B_{n,k}\right)}{\sigma_A}\right)^2\right]\right\} \tag{47}$$

The criterion to optimize is then

$$C(X) = \sum_{\substack{i=1 \\ i\neq i_0}}^{N_S}\sum_{k=1}^{K} C_1(X|\Delta r_{i,k}, R_{i,k}) + \sum_{l=1}^{N_A}\sum_{k=1}^{K} C_2(X|c^D_{l,k}, R^D_{l,k}) + \sum_{n=1}^{N_A}\sum_{k=1}^{K} C_3(X|c^B_{n,k}, R^B_{n,k}) \tag{48}$$

Fig. 3 presents an example of the measurements obtained from each sensor.

Remark: Following [6], we neglect the correlation between the TDOA measurements.

C. Numerical Computation and Optimization

All the methods explained hereafter are applied whatever the architecture (ML-PDA or ML-PDA with AI) is.

The maximization of the criterion is carried out by using a quasi-Newton (variable metric) method, as given in [12]. The aim is to compute an approximation of the inverse of the Hessian matrix. The update is done with the Davidon–Fletcher–Powell [17]–[19] method. The matrix is updated after each iteration of the algorithm. This guarantees that the matrix is symmetric and positive definite. The state is then updated employing the classical Newton–Raphson method:

$$\hat{X}_i = \hat{X}_{i-1} - p_i H_i^{-1} \nabla C(\hat{X}_i) \tag{49}$$

where H_i^{-1} is the approximation of the inverse of the Hessian matrix at step i and p_i is the optimal step-size scaling. Note that $\left(H_i^{-1}\right)_i$ converges to the inverse of the Hessian matrix.

The log-likelihood function being a highly non-convex and multi-modal function [2], [12], several techniques are used to perform the maximization of the criterion. Indeed, due to the multi-modality aspect, the algorithm could converge to a local maximum. To avoid this, a multi-pass approach was performed in [2] and will be now described.

This technique achieves the maximization in M steps instead of one. The algorithm is first initialized by a rough grid search method over the state space. At step m, instead of maximizing $C(X)$, the maximization is applied to $C^{(m)}(X)$, which is equal to $C(X)$ defined either by (44) or (48) where the standard deviations are multiplied by a_m (see [2], Section III). The numerical series a_m is decreasing such that $a_1 = M$, $a_2 = M-1$, ..., $a_M = 1$. The resulting state after maximization at step m is used as the initialization at step $m+1$. This method allows the algorithm to have a better 'sight' of the true detections, and ensures convergence towards the global maximum.

Moreover, to avoid convergence to an unrealistic state, a constraint (penalty function) $\phi(X)$ is added to $C^{(m)}(X)$ [2]. This penalty function is about the velocity of the target and is defined as follows:

$$\phi(X) = -\frac{1}{2}\left[\frac{v(X) - \bar{v}}{\sigma_v}\right]^2 \tag{50}$$

where

$$v(X) = \sqrt{X(4)^2 + X(5)^2} \tag{51}$$

$\bar{v}$ is a typical value of the target velocity and σ_v is the standard deviation around $\bar{v}$. At step $m = M$, the penalty function is relaxed.

D. The Fisher Information Matrix

An expression for the FIM in a clean environment is given in (35). In the presence of clutter, the computation of the FIM will use the statistical assumptions of the ML-PDA model. First, the measurement space is restricted to a gate around the true measurements [2], [8]. The size of the gate[3] is denoted by v_g:

[3]For a one-dimensional measurement.

$$v_g = 2g\sigma \tag{52}$$

The restriction to a gate around the true measurements allows the inclusion of only the most informative measurements. Indeed, with $g = 5$, more than 99% of a Gaussian population is within 5 standard deviations of the mean. The measurements located outside the gate contain no additional information about the state vector. By using these assumptions as well as the likelihood computed only with the measurements inside the gate, it is possible to find an expression for the FIM in the presence of clutter. Then, the latter appears to be the FIM in a clean environment multiplied by a scalar factor: the information reduction factor.

This factor, called q_2 in the literature on the ML-PDA architecture and q_3 in the ML-PDA with AI architecture, lies between 0 and 1 and represents the loss of information due to the presence of clutter and the non-unity detection probability [2], [8]. The information reduction factor only depends on P_d and λv_g, the expected number of false alarms in the gate of size v_g. It is then clear that the loss of information will increase the CRLB. Here are expressions for q_2 and q_3:

$$q_2(\lambda v_g, P_d) = \sum_{m=1}^{\infty} \frac{2P_d}{\sqrt{2\pi} g^{m-1}} \mu_{fa}(m-1) \times \int_0^g \cdots \int_0^g \frac{\exp(-\xi_1^2)\xi_1^2}{\frac{(1-P_d)\sqrt{2\pi}\lambda v_g}{2gP_d} + \sum_{i=1}^{m} \exp\left(-\frac{1}{2}\xi_i^2\right)} d\xi_1 \cdots d\xi_m \tag{53}$$

$$q_3(\lambda v_g, P_d) = \sum_{m=1}^{\infty} \frac{2P_d}{\sqrt{2\pi} g^{m-1}} \mu_{fa}(m-1) \times \int_0^g \cdots \int_0^g \int_\tau^\infty \cdots \int_\tau^\infty \frac{\prod_{j=1}^{m} p_0^\tau(R_j)\rho_1^2 \exp\left(-\xi_1^2\right)\xi_1^2}{\frac{(1-P_d)\sqrt{2\pi}\lambda v_g}{2gP_d} + \sum_{j=1}^{m} \rho_j \exp\left(-\frac{1}{2}\xi_j^2\right)} \times dR_1 \cdots dR_m d\xi_1 \cdots d\xi_m \tag{54}$$

The derivation of q_2 is detailed in [2] and in [9], where it is generalized to a multi-dimensional measurement. The derivation of the q_3 is given in Appendix A, based on [11], [12].

Then, it is possible to express the FIM in the presence of clutter in both architectures:

$$F_1 = q_2(\lambda_\Delta 2g\sigma_\Delta, P_{d\Delta})F_\Delta + q_2(\lambda_A 2g\sigma_A, P_{dA})F_A \tag{55}$$

$$F_2 = q_3(\lambda_\Delta 2g\sigma_\Delta, P_{d\Delta})F_\Delta + q_3(\lambda_A 2g\sigma_A, P_{dA})F_A \tag{56}$$

where F_1 and F_2 are the FIM in ML-PDA and ML-PDA with AI architectures respectively.

These factors are computed numerically by using Monte Carlo runs [20].

E. Test for Track Acceptance

Once the algorithm returns an estimate, it is necessary to decide if the estimated track is correct or not. Indeed, whether there is a target or not, the algorithm computes an estimate. If there is no correct detection, the estimate must be rejected as well as when the algorithm converges towards a local maximum. So we have to choose between two hypotheses:

- H_0: There is a track and $\hat{X}$ is the global maximum of the likelihood function.
- H_1: There is no track, or $\hat{X}$ is a local maximum.

The natural reflex would be to use the so-called generalized likelihood ratio (GLR) to construct a test between these two hypotheses. This needs the statistical distributions of the GLR (or a monotonic function of it) under each hypothesis. Determining these distributions is a tough task (from [2], Section IV, "the statistical distribution of [the GLR] is not available"). Following [2], we propose the palliative described below to circumvent this. We give the details for the case where the amplitude information is not available. We consider the following statistic[4]:

$$T_{0,1}(\hat{X}) = \frac{T_1 + T_2 + T_3}{\sqrt{V_1 + V_2 + V_3}} \tag{57}$$

with

$$T_1 = \sum_{\substack{i=1 \\ i \neq i_0}}^{N_S} \sum_{k=1}^{K} \left\{ C_1\left(\hat{X}|\Delta r_{i,k}^*\right) - \mathrm{E}\left[C_1\left(\hat{X}|\Delta r_{i,k}^*\right)|H_0\right] \right\} \tag{58}$$

$$T_2 = \sum_{l=1}^{N_A} \sum_{k=1}^{K} \left\{ C_2\left(\hat{X}|c_{l,k}^{D,*}\right) - \mathrm{E}\left[C_2\left(\hat{X}|c_{l,k}^{D,*}\right)|H_0\right] \right\} \tag{59}$$

$$T_3 = \sum_{n=1}^{N_A} \sum_{k=1}^{K} \left\{ C_3\left(\hat{X}|c_{l,k}^{B,*}\right) - \mathrm{E}\left[C_3\left(\hat{X}|c_{l,k}^{B,*}\right)|H_0\right] \right\} \tag{60}$$

$$V_1 = \sum_{\substack{i=1 \\ i \neq i_0}}^{N_S} \sum_{k=1}^{K} \mathrm{Var}\left[C_1\left(\hat{X}|\Delta r_{i,k}^*\right)|H_0\right] \tag{61}$$

$$V_2 = \sum_{l=1}^{N_A} \sum_{k=1}^{K} \mathrm{Var}\left[C_2\left(\hat{X}|c_{l,k}^{D,*}\right)|H_0\right] \tag{62}$$

$$V_3 = \sum_{l=1}^{N_A} \sum_{k=1}^{K} \mathrm{Var}\left[C_3\left(\hat{X}|c_{l,k}^{B,*}\right)|H_0\right] \tag{63}$$

Since $\hat{X}$ is supposed to be the global maximum, we get the following approximations.

$$\mathrm{E}\left[C_1\left(\hat{X}|\Delta r_{i,k}^*\right)|H_0\right] \simeq \mathrm{E}\left[C_1\left(X|\Delta r_{i,k}^*\right)|H_0\right] = \mu_{0,1} \tag{64}$$

$$\mathrm{E}\left[C_2\left(\hat{X}|c_{l,k}^{D,*}\right)|H_0\right] \simeq \mathrm{E}\left[C_2\left(X|c_{l,k}^{D,*}\right)|H_0\right] = \mu_{0,2} \tag{65}$$

$$\mathrm{E}\left[C_3\left(\hat{X}|c_{l,k}^{B,*}\right)|H_0\right] \simeq \mathrm{E}\left[C_3\left(X|c_{l,k}^{B,*}\right)|H_0\right] = \mu_{0,3} \tag{66}$$

[4] $*$ is for the measurements inside the gate.

$$\mathrm{Var}\left[C_1\left(\hat{X}|\Delta r_{i,k}^*\right)|H_0\right] \simeq \mathrm{Var}\left[C_1\left(X|\Delta r_{i,k}^*\right)|H_0\right] = \sigma_{0,1}^2 \tag{67}$$

$$\mathrm{Var}\left[C_2\left(\hat{X}|c_{l,k}^{D,*}\right)|H_0\right] \simeq \mathrm{Var}\left[C_2\left(X|c_{l,k}^{D,*}\right)|H_0\right] = \sigma_{0,2}^2 \tag{68}$$

$$\mathrm{Var}\left[C_3\left(\hat{X}|c_{l,k}^{B,*}\right)|H_0\right] \simeq \mathrm{Var}\left[C_3\left(X|c_{l,k}^{B,*}\right)|H_0\right] = \sigma_{0,3}^2 \tag{69}$$

The statistic (57) can be rewritten as

$$T_{0,1}(\hat{X}) = \frac{C(\hat{X}) - (N_S - 1)K\mu_{0,1} - N_A K(\mu_{0,2} + \mu_{0,3})}{\sqrt{(N_S - 1)K\sigma_{0,1}^2 + N_A K(\sigma_{0,2}^2 + \sigma_{0,3}^2)}} \tag{70}$$

It has been shown empirically that $T_{0,1}$ follows the standard Gaussian distribution by using the Central Limit Theorem [2]. With all these considerations, the test is the following: if $T_{0,1} > c_\alpha$ H_0, is accepted. Otherwise, H_0 is rejected. c_α is then the threshold with a level of significance α.

When the amplitude information is available, only the values of $\mu_{0,i}$ and $\sigma_{0,i}$ will change. The expressions for $\mu_{0,i}$ and $\sigma_{0,i}$ are detailed in [2], [9] for the ML-PDA architecture and in Appendix B for the ML-PDA with AI architecture.

VI. Numerical Results

In this section, some numerical results of the estimator are presented.

A. Results in ML-PDA Model

We first present the numerical results obtained for the ML-PDA architecture in different configurations. The following assumptions are made:

- $P_d = P_{d\Delta} = P_{dA}$
- λ_Δ and λ_A are set such that the expected number of false alarms λu is the same for each sensor.

Each configuration is defined by specific values of $(P_d; \lambda u)$ and by the specific positions of the sensors (according to the uniform law in a square with sides of 20 km). We recall that the number of sampling times is $K = 100$. Then, 200 Monte Carlo runs are performed for each configuration. The results of the Monte Carlo runs are presented in Tables II and III. $\bar{X}$ is the mean of the estimates. The mean value of the NEES[5] [8] is computed. For 200 simulations, and a 5-dimensional parameter, the confidence interval of the NEES at 95% is $[4.55; 5.45]$. In each configuration, the NEES is close to the theoretical value (5) and belongs to the confidence region. This indicates that the estimator is efficient, that is, unbiased and meeting the CRLB.

B. Results in ML-PDA with AI Model

As we use the AI, we have to define the pdf of the amplitude under both hypotheses. It is assumed that the energy of the background noise follows a central χ_2^2 distribution, and the target originated signal follows a non-central χ_2^2 distribution. The non-centrality parameter depends on the SNR, which is

[5] Normalized Estimation Error Square.

TABLE II
RESULTS OF 200 MONTE CARLO RUNS WITH ML-PDA ARCHITECTURE FOR THE SLOW TARGET ($X = X_L$)

$(P_d; \lambda u)$	$(0.8; 2)$	$(0.6; 8)$
$\bar{x}$	-5004	-5005.5
$\bar{y}$	2998.9	2995.6
$\bar{z}$	-298.09	-298.55
$\bar{\dot{x}}$	4.036	4.013
$\bar{\dot{y}}$	3.015	3.010
$\overline{\text{NEES}}$	5.39	5.37
Acceptance rate	94.5%	84%

TABLE III
RESULTS OF 200 MONTE CARLO RUNS WITH ML-PDA ARCHITECTURE FOR THE FAST TARGET ($X = X_H$)

$(P_d; \lambda u)$	$(0.9; 2)$	$(0.8; 6)$	$(0.6; 8)$
$\bar{x}$	-5001.7	-5004.4	-4918.9
$\bar{y}$	2999.1	2999.3	3013.8
$\bar{z}$	-299.77	-300.69	-298.03
$\bar{\dot{x}}$	24.993	25.011	24.936
$\bar{\dot{y}}$	11.999	12.002	11.958
$\overline{\text{NEES}}$	5.18	5.13	5.36
Acceptance rate	96.5%	94%	93%

TABLE IV
RESULTS OF 100 MONTE CARLO RUNS WITH ML-PDA WITH AI ARCHITECTURE FOR THE SLOW TARGET ($X = X_L$)

$\bar{X}$	$\overline{\text{NEES}}$	Acceptance rate
$(-5005.9; 2995.5; -303.39; 4.069; 3.043)$	5.48	99%

TABLE V
RESULTS OF 100 MONTE CARLO RUNS WITH ML-PDA WITH AI ARCHITECTURE FOR THE FAST TARGET ($X = X_H$)

$\bar{X}$	$\overline{\text{NEES}}$	Acceptance rate
$(-4999.2; 3002.7; -300.19; 24.997; 11.990)$	5.01	99%

low. The detection threshold is placed such that $P_{fa} = 0.02$ and $P_d = 0.6$. The value of K is still 100.

For this configuration, 100 Monte Carlo runs are performed. The result of these runs is shown in Tables IV and V. The 95% confidence interval of the NEES for 100 simulations is $[4.37; 5.63]$. The mean value of the NEES is in the confidence interval and near the theoretical value of 5. Hence, the estimator is efficient.

VII. CONCLUSION

In this paper, we treated the problem of estimating the trajectory of a source in CV motion when the available measurements are a set of TDOA provided by a sonobuoy network, and the cosines of elevation angles acquired by vertical antennas. To begin with, the observability was studied before proposing an estimate. Then, we chose a convenient model for noisy measurements. Due to the simplicity of the system embarked in a sonobuoy (which performs very basic signal processing functions such as thresholding the signal energy), the data were assumed to be composed of correct detections and false alarms. Consequently, we employed the PDA model, well adapted to this situation. The proposed estimator (the MLE) was found to be efficient (the empirical covariance matrix reaches the CRLB) even with only three sonobuoys and two vertical linear arrays. Coupling their energy to these thresholded data improve the accuracy of the MLE, which remains efficient in this case. Nevertheless, two points were neglected: the propagation delay of the waves carrying the signal, and the correlation between the TDOA measurements. Future research will be focused on these two points.

APPENDIX A
DERIVATION OF THE INFORMATION REDUCTION FACTOR q_3

We derive q_3 according to the principles detailed in [2], [9], [11], [12]. We first express the likelihood at time k by considering only the measurements inside the gate of size v_g. We use the same notation as in Section III.

$$\begin{aligned} L(X|s) = &\frac{1-P_d}{u^m}\mu_{fa}(m)\prod_{i=1}^{m} p_0^\tau(R_i) \\ &+ \frac{P_d}{u^{m-1}}\frac{\mu_{fa}(m-1)}{m}\prod_{i=1}^{m} p_0^\tau(R_i) \\ &\times \sum_{i=1}^{m}\frac{1}{\sqrt{2\pi}\sigma}\rho_i \exp\left[-\frac{1}{2}\left(\frac{s_i - h(X)}{\sigma}\right)^2\right] \end{aligned} \tag{71}$$

After factorization we get

$$\begin{aligned} L(X|s) = &\frac{\mu_{fa}(m)}{v_g^m}\prod_{i=1}^{m} p_0^\tau(R_i)\left\{1 - P_d + \frac{P_d}{\lambda}\right. \\ &\left.\times \sum_{i=1}^{m}\frac{1}{\sqrt{2\pi}\sigma}\rho_i \exp\left[-\frac{1}{2}\left(\frac{s_i - h(X)}{\sigma}\right)^2\right]\right\} \end{aligned} \tag{72}$$

We define

$$\Phi(X|s) = 1 - P_d + \frac{P_d}{\lambda}\sum_{i=1}^{m}\frac{\rho_i}{\sqrt{2\pi}\sigma}\exp\left[-\frac{1}{2}\left(\frac{s_i - h(X)}{\sigma}\right)^2\right] \tag{73}$$

Then, the information reduction factor q_3 is

$$\begin{aligned} q_3 = &\sum_{m=1}^{\infty}\frac{1}{2\pi\sigma^2}\left(\frac{P_d}{\lambda}\right)^2\frac{\mu_{fa}(m)}{v_g^m} \\ &\times \int_{-g}^{g}\cdots\int_{-g}^{g}\int_{\tau}^{\infty}\cdots\int_{\tau}^{\infty}\frac{\prod_{i=1}^{m} p_0^\tau(R_i)}{\Phi(X|s)} \\ &\times \sum_{i=1}^{m}\sum_{j=1}^{m}\rho_i\rho_j \exp\left[-\frac{1}{2}\left(\frac{s_i - h(X)}{\sigma}\right)^2\right. \\ &\left.-\frac{1}{2}\left(\frac{s_j - h(X)}{\sigma}\right)^2\right]\frac{s_i - h(X)}{\sigma}\frac{s_j - h(X)}{\sigma} \\ &\times dR_1\cdots dR_m ds_1\cdots ds_m \end{aligned} \tag{74}$$

We define

$$\xi_i = \frac{s_i - h(X)}{\sigma} \tag{75}$$

$$a = 1 - P_d \tag{76}$$

$$b = \frac{1}{\sqrt{2\pi}\sigma}\frac{P_d}{\lambda} \tag{77}$$

Reintroducing in (74) these notations, we obtain

$$\begin{aligned} q_3 = &\sum_{m=1}^{\infty} b^2 \frac{\mu_{fa}(m)}{v_g^m} \\ &\times \int_{v_g}\cdots\int_{v_g}\int_{\tau}^{\infty}\cdots\int_{\tau}^{\infty} \frac{\prod_{i=1}^m p_0^\tau(R_i)}{a + b\sum_{i=1}^m \rho_i \exp(-\frac{1}{2}\xi_i^2)} \\ &\cdot \sum_{i=1}^m \sum_{j=1}^m \rho_i\rho_j \exp\left[-\frac{1}{2}\xi_i^2 - \frac{1}{2}\xi_j^2\right]\xi_i\xi_j \\ &\times dR_1\cdots dR_m d\xi_1\cdots d\xi_m \end{aligned} \tag{78}$$

Then, we use the following principles to simplify the expression for q_3: it is an odd function with respect to ξ_i for ξ_j fixed. The cross terms then vanish from the integrals. Next, we use the parity of the function with respect to ξ_i. After some manipulations, we finally obtain the expression given in (54).

APPENDIX B
DERIVATION OF THE MOMENTS OF THE LOG-LIKELIHOOD FUNCTION UNDER TARGET HYPOTHESIS IN ML-PDA WITH AI

We derive $\mu_0^{(n)}$ in the ML-PDA architecture. The derivation is based upon [11], [12]. The criterion is the following:

$$\begin{aligned} C(X|s) = \log\Bigg\{1 - P_d + \frac{P_d}{\lambda} \\ \sum_{i=1}^m \frac{1}{\sqrt{2\pi}\sigma}\rho_i \exp\left[-\frac{1}{2}\left(\frac{s_i - h(X)}{\sigma}\right)^2\right]\Bigg\} \end{aligned} \tag{79}$$

We want to compute (80) with the likelihood given in (71):

$$\mu_0^{(n)} = \sum_{m=0}^{\infty}\int_{v_g}\cdots\int_{v_g} (C(X|s))^n L(X|s) ds_1\cdots ds_m \tag{80}$$

For $m = 0$ we have

$$\mu_0^{(n)}(0) = (1 - P_d)\exp(-\lambda v_g)\log^n(1 - P_d) \tag{81}$$

We use the same change of variables given in (75), (76), (77) and we get

$$\begin{aligned} \mu_0^{(n)} = \mu_0^{(n)}(0) + &\sum_{m=1}^{\infty}\int_{-g}^{g}\cdots\int_{-g}^{g}\int_{\tau}^{\infty}\cdots\int_{\tau}^{\infty} \sigma^m \frac{\mu_{fa}(m)}{v_g^m} \\ &\times \log^n\left(a + b\sum_{i=1}^m \rho_i \exp\left[-\frac{1}{2}\xi_i^2\right]\right) \\ &\times \prod_{i=1}^m p_0^\tau(R_i)\left(a + b\sum_{i=1}^m \rho_i \exp\left[-\frac{1}{2}\xi_i^2\right]\right) \\ &\times dR_1\cdots dR_m d\xi_1\cdots d\xi_m \end{aligned} \tag{82}$$

We then use the parity with respect to ξ_i and notice that the integrals are the same for each considered index. After some manipulations we get

$$\begin{aligned} \mu_0^{(n)} = \mu_0^{(n)}(0) + &\sum_{m=1}^{\infty}\int_{0}^{g}\cdots\int_{0}^{g}\int_{\tau}^{\infty}\cdots\int_{\tau}^{\infty} \frac{2P_d\mu_{fa}(m)}{g^{m-1}\lambda v_g\sqrt{2\pi}} \\ &\times \log^n\left(a + b\sum_{i=1}^m \rho_i \exp\left[-\frac{1}{2}\xi_i^2\right]\right) \\ &\times \prod_{i=1}^m p_0^\tau(R_i)\left(\frac{(1-P_d)\sqrt{2\pi}\lambda v_g}{2gP_d} + m\rho_1 \exp\left[-\frac{1}{2}\xi_1^2\right]\right) \\ &\times dR_1\cdots dR_m d\xi_1\cdots d\xi_m \end{aligned} \tag{83}$$

REFERENCES

[1] R. W. Sittler, "An optimal data association problem in surveillance theory," *IEEE Transactions on Military Electronics*, vol. 8, no. 2, pp. 125–139, Apr. 1964.

[2] C. Jauffret and Y. Bar-Shalom, "Track formation with bearing and frequency measurements in clutter," *IEEE Transactions on Aerospace and Electronic Systems*, vol. 26, no. 6, pp. 999–1010, 1990.

[3] R. J. Urick, *Principles of Underwater Sound*. New York: McGraw-Hill, 1975.

[4] J. Arnold, Y. Bar-Shalom, R. Estrada, and R. Mucci, "Target parameter estimation using measurements acquired with a small number of sensors," *IEEE Journal of Oceanic Engineering*, vol. 8, no. 3, pp. 163–172, 1983.

[5] H. L. Van Trees, *Detection, Estimation, and Modulation Theory, Part I*. Wiley, 2004.

[6] K. W. Lo and B. G. Ferguson, "Broadband passive acoustic technique for target motion parameter estimation," *IEEE Transactions on Aerospace and Electronic Systems*, vol. 36, no. 1, pp. 163–175, 2000.

[7] Y. Bar-Shalom and E. Tse, "Tracking in a cluttered environment with probabilistic data association," *Automatica*, vol. 11, no. 5, pp. 451–460, 1975.

[8] Y. Bar-Shalom and T. Fortmann, *Tracking and Data Association*. Academic Press, 1988.

[9] C. Jauffret, "Trajectographie passive, observabilité et prise en compte des fausses alarmes," Ph.D. dissertation, Toulon, 1993.

[10] D. Ciuonzo, P. K. Willett, and Y. Bar-Shalom, "Tracking the tracker from its passive sonar ML-PDA estimates," *IEEE Transactions on Aerospace and Electronic Systems*, vol. 50, no. 1, pp. 573–590, 2014.

[11] T. Kirubarajan, Y. Bar-Shalom, and Y. Wang, "Passive ranging of a low observable ballistic missile in a gravitational field," *IEEE Transactions on Aerospace and Electronic Systems*, vol. 37, no. 2, pp. 481–494, 2001.

[12] T. Kirubarajan and Y. Bar-Shalom, "Low observable target motion analysis using amplitude information," *IEEE Transactions on Aerospace and Electronic Systems*, vol. 32, no. 4, pp. 1367–1384, 1996.

[13] P. Blanc-Benon and C. Jauffret, "TMA from bearings and multipath time delays," *IEEE Transactions on Aerospace and Electronic Systems*, vol. 33, no. 3, pp. 813–824, 1997.

[14] K. F. Gong, "Multipath target motion analysis: Properties and implication of the multipath process." 6687, NUSC, Newport, RI, Tech. Rep., 1982.

[15] R. Moose and T. Dailey, "Adaptive underwater target tracking using passive multipath time-delay measurements," *IEEE transactions on acoustics, speech, and signal processing*, vol. 33, no. 4, pp. 778–787, 1985.

[16] A.-C. Pérez and C. Jauffret, "Observability in target motion analysis from the sum or the difference of ranges with two stationary sensors," in *2020 IEEE 23rd International Conference on Information Fusion (FUSION)*, 2020, pp. 1–8.

[17] M. L. Lenard, "Practical convergence conditions for the Davidon–Fletcher–Powell method," *Mathematical Programming*, vol. 9, no. 1, pp. 69–86, 1975.

[18] R. Fletcher and M. J. Powell, "A rapidly convergent descent method for minimization," *The Computer Journal*, vol. 6, no. 2, pp. 163–168, 1963.

[19] W. C. Davidon, "Variable metric method for minimization," *SIAM Journal on Optimization*, vol. 1, no. 1, pp. 1–17, 1991.

[20] C. Robert, *L'analyse statistique bayésienne*. Economica, 1992.

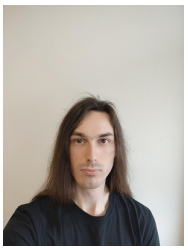

Jérémy Payan was born in Toulon, France in 1997. He received his masters degree "Vision Signal Trajectographie Automatique" from the Université de Toulon, France in 2019.

He is currently pursuing a Ph.D. degree in signal processing in the Université de Toulon, France, with the french laboratory IM2NP, and with the company Naval Group Research, Ollioules, France. His work is about target motion analysis methods for passive sonar systems.

Antoine Lebon was born in Briey, France in 1994. He received his masters degree "signal et trajectographie" from the Université de Toulon, France in 2018.

He is currently pursuing a Ph.D. degree in signal processing in the Université de Toulon, France, with the french laboratory IM2NP, and with the company Naval Group Research, Ollioules, France. His work is about target motion analysis methods for passive sonar systems.

Annie-Claude Pérez was born in France on November 10, 1965, received the Diplôme d'Etudes Appronfondies in Optics and Image Processing, from the Université de Toulon, France, in 1988, and the title of "Docteur de l'Université" in 1991 from the Université de Toulon, France.

Since Sept. 1994, she has been at the University de Toulon, where she teaches electronic systems. Her research is focused on signal processing, applied to biomedical systems before turning them to target motion analysis.

Claude Jauffret was born in France on March 29, 1957, and received the Diplôme d'Etudes Appronfondies in Applied Mathematics, from Saint Charles University, Marseille, France, in 1981, the Diplôme d'Ingénieur from Ecole Nationale Supérieure d'Informatique et de Mathématiques Appliqués de Grenoble, Grenoble, France, in 1983, the title of "Docteur de l'Université" in 1993, and the "Habilitation à Diriger des Recherches" from the Université de Toulon, France.

From November 1983 to November 1988, he worked on passive sonar systems, more precisely, on target motion analysis at GERDSM, France. After a sabbatical year at the University of Connecticut (from November 1988 to December 1989), during which he worked on tracking problems in a cluttered environment, he developed research in tracking, data fusion, and extraction in CERDSM. Since Sept. 1996, he has been at the Université de Toulon, where he teaches statistical signal processing. His current research is about observability and estimation in nonlinear systems, as it appears in tracking problems.

Dann Laneuville graduated from "Ecole Supérieure d'Electricité" (a.k.a. Supélec) in 1987 and got a Ph.D. in automatic and signal processing from the Paris XI Orsay University in 1998. He is currently R& D engineer in the Advanced Algorithms and Architectures department within Naval Group Research, Naval Group's research and technology centre based in Nantes, France. Before joining Naval Group in 2003, he has been for ten years within the Image and Signal Processing Laboratory of Matra Group and with MBDA's department of guidance and control for five years. Before joining Naval Group Research at its creation in 2012, he has spent a year as a visiting scholar within the Electrical and Computing Engineering department at the University of Connecticut where he studied maneuvering target tracking and video extraction algorithms. He has published over forty papers in international renowned conferences and workshops (Conference on Decision and Control, Aerospace Conference, International Conference on Information Fusion, IET seminar, SDF workshop, MAST, UDT...), been a key actor during fifteen years within the "collège de Polytechnique" multisensor fusion seminar. His areas of interest are multitarget tracking, maneuvering target tracking, bearing only tracking and data fusion.